1. Report No. FHWA/TX-06/0-4820-3	2. Government Accession No.	3. Recipient's Catalog No.
4. Title and Subtitle Investigation of a New Generation of FCC Compliant NDT Devices for Pavement Layer Information Collection: Technical Report		5. Report Date February 2006 Published: July 2006 6. Performing Organization Code
7. Author(s) Richard Liu, Jing Li, Xuemin Chen, Aditya Ekbote, Huichun Xing, and Ying Wang		8. Performing Organization Report No. 0-4820-3
9. Performing Organization Name and Address Department of Electrical and Computer Engineering, University of Houston, 4800 Calhoun Rd., Houston, TX 77204-4005		10. Work Unit No. 11. Contract or Grant No. 0-4820
12. Sponsoring Agency Name and Address Texas Department of Transportation Research and Technology Implementation Office P. O. Box 5080 Austin, TX 78763-5080		13. Type of Report and Period Covered Technical Report September 1, 2003 – August 31, 2005 14. Sponsoring Agency Code

15. Supplementary Notes
Project performed in cooperation with the Texas Department of Transportation and the Federal Highway Administration.
Project title: Investigation of a New Generation of FCC Compliant NDT Devices for Pavement Layer Information Collection
URL: http://tti.tamu.edu/documents/0-4820-3.pdf

16. Abstract:

To comply with the Federal Communications Commission (FCC) rules on the ground-penetrating radar (GPR) devices, the first stage of the project has investigated methodologies to avoid FCC banned frequency bands, and developed a hybrid GPR system that utilizes two separate frequency bands, DC-960MHz and 3.1GHz-8.5GHz. The detailed information of this system can be found in the reports 0-4820-1 and 0-4820-2 of this project. This report will concentrate on the air launching version of the pulse GPR, including new air launching antenna design, signal processing, and subsurface layer information extraction from GPR raw data. A lot of lab tests have been performed. Field tests have been conducted on TTI Annex, FM2818, Texas Avenue, and SH21 in College Station and Bryan, respectively. The measured results agree with the real cases very well. The developed GPR system is able to collect pavement layer information accurately and in real time. The system is completely ready for implementation.

17. Key Words FCC Rules on GPR, FCC-Compliant GPR, Pavement Thickness and Dielectric Constant Measurement, Network Level Layer Information Collection		18. Distribution Statement No restrictions. This document is available to the public through National Technical Information Service, Springfield, Virginia, 22161, www.ntis.gov.	
19. Security Classif. (of this report) Unclassified	20. Security Classif. (of this page) Unclassified	21. No. of Pages 28	22. Price

Form DOT F 1700.7 (8-72)
This form was electrically by Elite Federal Forms Inc.

Investigation of a New Generation of FCC Compliant NDT Devices for Pavement Layer Information Collection: Technical Report

by

Richard Liu, Jing Li, Xuemin Chen, Aditya Ekbote, Huichun Xing, and Ying Wang

Technical Report 0-4820-3

Project Number: 0-4820
Project Title: Investigation of a New Generation of FCC Compliant NDT Devices for Pavement Layer Information Collection

Performed in Cooperation with the
Texas Department of Transportation
and the
Federal Highway Administration

by the

Subsurface Sensing Laboratory
Department of Electrical and Computer Engineering
University of Houston

February 2006
Published: July 2006

DISCLAIMERS

University of Houston
4800 Calhoun Rd.
Houston, TX 77204

ACKNOWLEDGEMENTS

This project was sponsored by the Texas Department of Transportation. The research work was greatly supported by: the Project Director, Brian Michalk; the Program Coordinator, Ed Oshinski; and the TxDOT Research Engineer, Dr. German Claros.

Table of Contents

List of Figures

CHAPTER 1: INTRODUCTION

After FCC adopted a new rule on GPR devices on July 12, 2002, that permits the operation of GPRs and wall imaging systems only below 960 MHz or between 3.1 and 10.6 GHz, a hybrid GPR system has been developed that is composed of two individual subsystems: 1) a pulse GPR radar working in the frequency range from DC to 900 MHz for thick pavement layers and subgrade layers detection, and 2) a frequency-modulated-continuous-wave (FMCW) radar working in the frequency range from 3.1GHZ to 8.5 GHz for measuring thin asphalt layers. This system is verified to be able to detect pavement layer thickness and dielectric constant [1]. However, the developed low frequency pulse GPR works in the ground coupling mode, which requires GPR antenna be very close to the pavement surface and hence limits the measurement speed. In this stage, a new air launching version of the pulse GPR is developed. Because the air launching GPR can be mounted on a vehicle and high above the pavement surface, the measurement can be made at highway speed. This report will mainly introduce the design and test of the air launching version pulse GPR. In Chapter 2, the structure and the features of air-coupled antennas will be introduced. In the ground coupling version, the wideband bowtie antennas are used to enhance the ground coupling effect, but in the air-coupled version, we need highly directional wideband antennas that have high radiation efficiency. Chapter 3 will talk about the elimination of the background noises for air-coupled GPR. The low frequency pulsed GPR radiates relatively wide pulse waves. The pavement-reflected signals will overlap with the later part of the transmitted waves, arousing difficulties in subsurface layer information extraction. The algorithms for eliminating the direct waves from measured GPR data are introduced in this chapter. The field test data of the air launching system will be given in Chapter 4. Conclusions and recommendations will be delivered in Chapter 5.

CHAPTER 2: TEM HORN ANTENNAS FOR AIR-COUPLED PULSE GPR

2.1 Air-coupled Pulse GPR

The hardware of an air-coupled pulse GPR is constructed exactly the same way as the ground-coupling pulse GPR as illustrated in [1]. It consists of a transmitter, a receiver, a control circuit unit, a host computer, a data acquisition circuit and two sets of wideband antennas. The working principle and procedures are illustrated in the block diagram shown in Fig. 2-1, where the components in the red-dashed-line box form the transmitter, the components in the green-dashed-line box make a receiver, and the clock is shared by both the transmitter and receiver. Whenever the GPR is turned on, the host computer will send a command to the control unit, and the control unit will trigger the transmitter to emit a short pulse wave into space via the transmitting antenna; at the same time, the control unit also sends a command to the sampling unit to pick up the incoming reflected signals. The transmitted wave from the transmitting antenna usually propagates in all directions in space, and part of it penetrates into the pavement. When the penetrated wave encounters the subsurface interface, it is reflected back and picked up by the receiving antenna. There is also another part of the transmitted wave propagating directly from the transmitting antenna to the receiving antenna or from the transmitting antenna to the pavement surface and then bouncing up to the receiving antenna, which is called the direct wave. The received direct wave and the subsurface reflected wave are both transferred to the host laptop by sampling unit and data acquisition card. By processing the received signals and finding travel time of reflected waves [2], the thickness, dielectric constant and moisture content of the pavement can be obtained and displayed.

What hardware in air-coupled GPR system differs from that in the ground-coupling GPR system are the antennas. Bowtie antennas have been used in the ground-coupling GPR system for their ultra wide band and high coupling efficiency with ground. But the antennas for air-coupled GPR should be directional with high radiation efficiency. Obviously the bowtie antenna does not belong to this category. Hence we turn to another type of ultra wide band antenna-TEM horn.

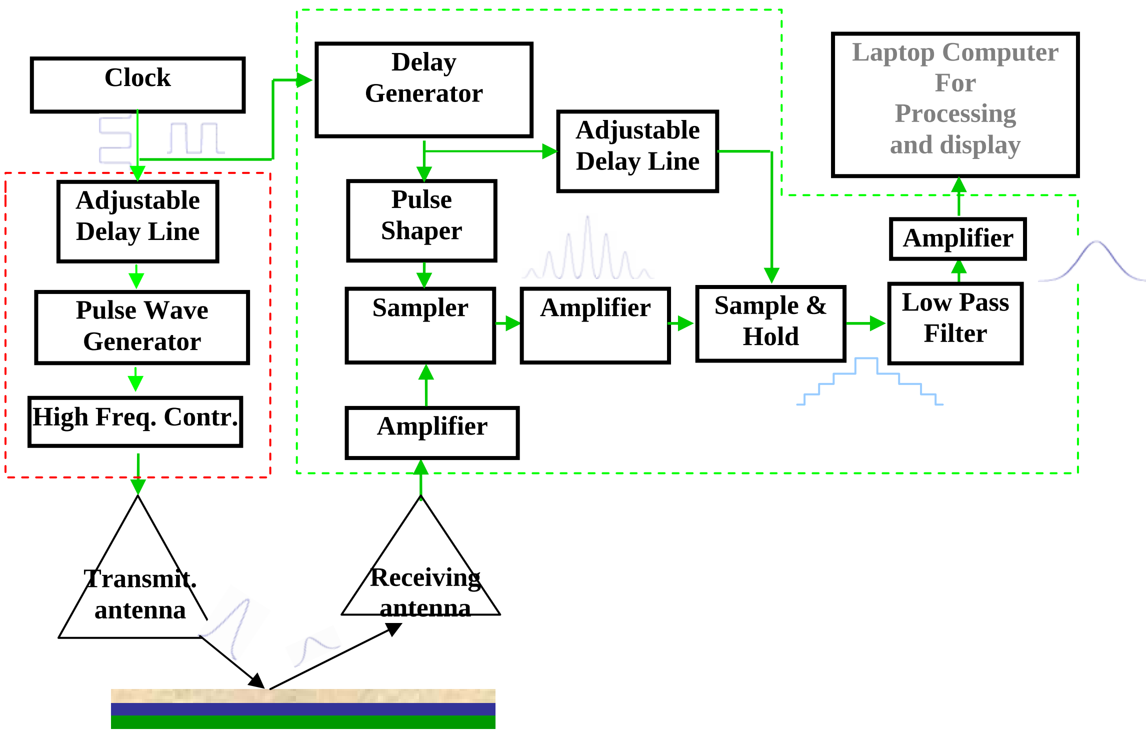

Fig. 2-1 Block diagram of the pulse GPR system

2.2 TEM Horn Antenna

A TEM horn antenna is made up of two symmetrical metal plates that are specially shaped, and the distance between two plates of the antenna is gradually increasing. Fig. 2-2 shows the front side of two fabricated TEM horn antennas bonded together, one antenna used for transmitting and the other one used for receiving.

The mechanism of the TEM horn antenna design is the "perfect" match of the transmission line impedance: the input impedance of the antenna at the top feeding point matches to that of the feeding coaxial cable; then the impedance of the antenna gradually increases along the antenna body until it reaches 377 Ohm at the open end of the antenna to match the wave impedance of free space; such that the microwave energy from the feeding coaxial cable can be smoothly transmitted into space without suffering critical reflection on the antenna. The shape of each metal plate and the flaring of the two plates of a TEM horn antenna are designed to minimize the reflections occurring along the antenna body [3]. This is the most important consideration that has to be made so that the wideband pulse can be effectively transmitted. If this design requirement is not accomplished, then the antenna will have fairly low radiation efficiency (as most of the pulse energy will be reflected from the antenna internally) as well as low directivity, two very important impulse radar antenna requirements. Therefore, this is the most important design consideration that has to be made when designing TEM horn antennas for impulse radar systems. According to the theory and calculated data in [3] and [4], the impedance and the dimensions of the TEM antenna can be calculated. Fig. 2-2 shows two antennas designed based on the theory in [4]. Fig. 2-3 gives the dimensions of the designed antenna plate.

Fig. 2-2 two TEM horn antennas

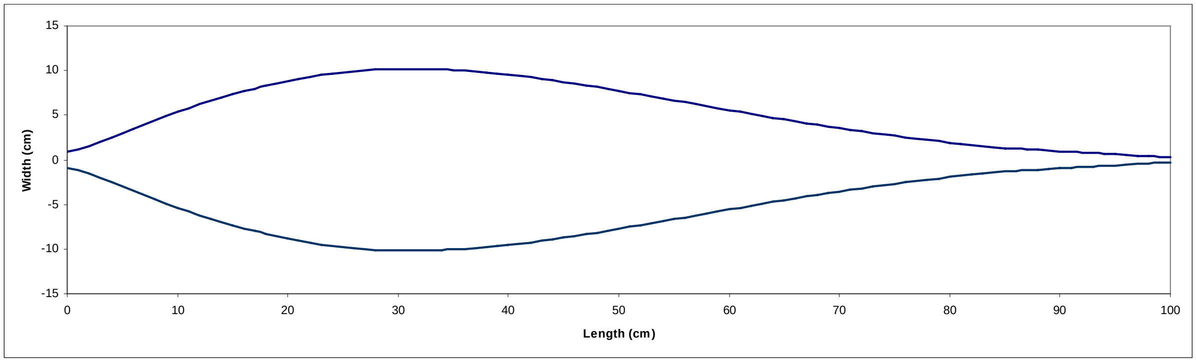

Fig. 2-3 Dimensions of the antenna plate

The measured reflection coefficient at the antenna input point is given in Fig. 2-4. From this figure, the working band is indeed very wide, covering a range from 100MHz to 3 GHz. It is wide enough to serve our pulse GPR.

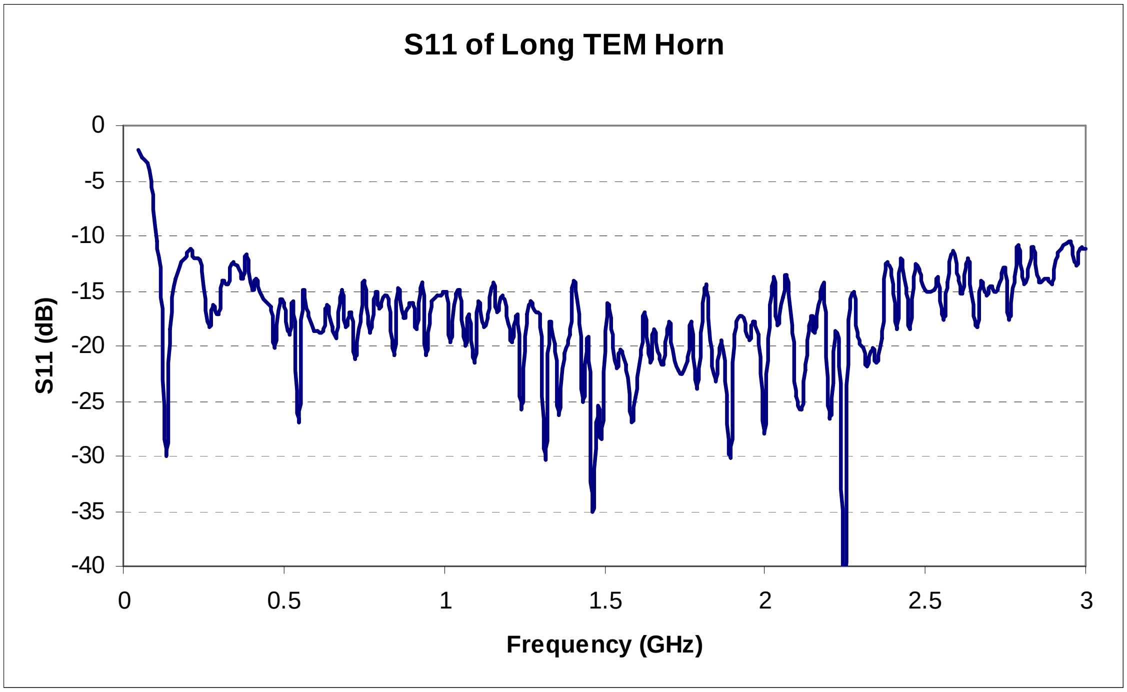

Fig. 2-4 Measured S11 of the developed TEM Horn antenna

By integrating the new TEM horn antennas to the previously developed pulse GPR system, an air-coupled version GPR is built. Fig. 2-5 shows the vehicle-mounted air-coupled pulse GPR developed. The lab tests verified that this GPR works properly.

However, this GPR system uses relatively low frequency pulse wave. The pavement layer reflected signals overlap with the rear part of the direct wave and hard to extract. Next chapter will discuss algorithms that help eliminate the interference for the direct waves.

Fig. 2-5Air-coupled version of the pulse GPR

CHAPTER 3 ELIMINATION OF THE BACKGROUND NOISES FOR AIR-COUPLED GPR

3.1 Influence of the Direct Waves

In order to comply with FCC rules, the width of a transmitted pulse should be relatively wide, greater than 3 ns. The rear part of the transmitted pulse wave will overlap with the reflected signals from shallow asphalt layers. Hence the rear part of the transmitted wave acts as strong noises to the received signals, which hinders the extraction of the pavement layer information from the measured GPR data. Fig. 3-1 is a typical received GPR color map and a waveform over an asphalt pavement.

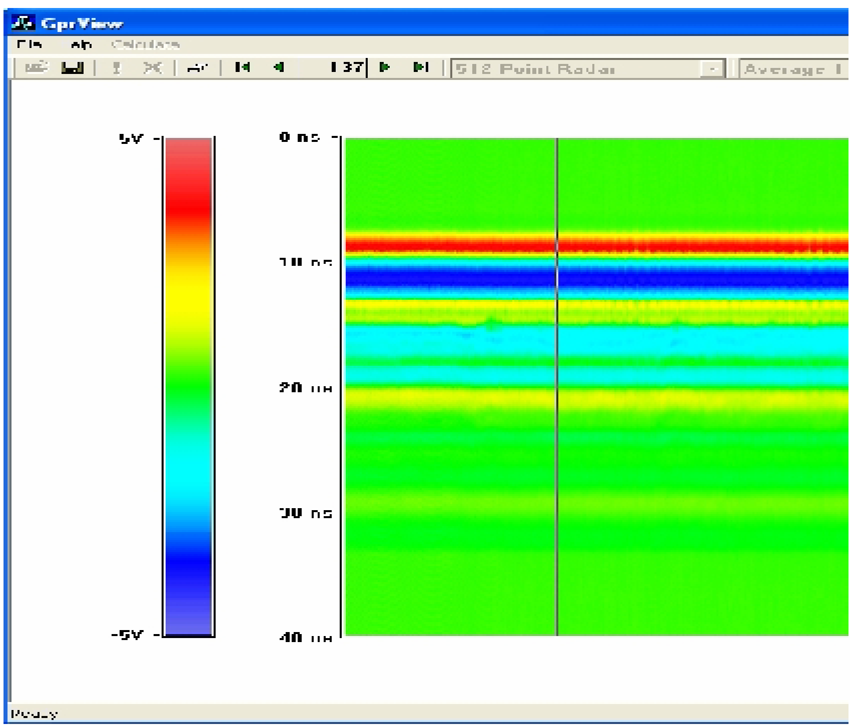

Fig. 3-1 A typical measured color map of low frequency pulse GPR

From this color map we see mainly the background noise or the directly-coupled waves. The subsurface information is not clear. In order to obtain accurate pavement layer information, data processing algorithms must be investigated.

3.2 Procedures of Data Processing for Air-coupled Pulse GPR

In air-coupled mode, the reflected signals from the subsurface layers are much weaker than that of the direct waves and background noises. Special techniques and algorithms must be employed to eliminate the interferences and extract the useful reflected signals. The most effective method is to subtract the direct waves and background noises from the measured signals. The procedures used in the air-coupled pulse GPR is described by the flow chart in Fig. 3-2.

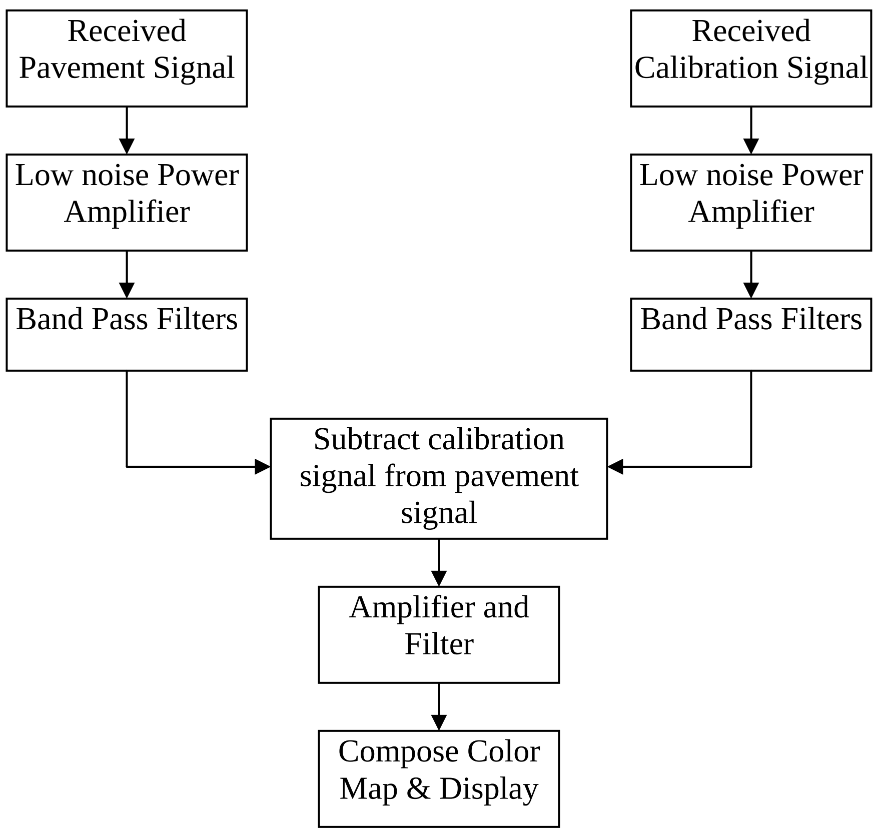

Fig. 3-2 Data processing procedures for air-coupled GPR

In Fig. 3-2, the calibration signal is obtained when a big metal plate is placed on the pavement right below the GPR antennas after the air launching GPR is setup on the vehicle. This calibration signal contains only the direct wave, the metal plate reflected wave and the background noises. It does not have any information of the subsurface pavement layers. After subtract this calibration signal, the measured waves over pavements will have only the surface reflection and subsurface layer reflections left. These useful signals are going to emerge in the new GPR color map. After applying the data processing algorithms to the data shown in Fig. 3-1, a new GPR color map is obtained as shown in Fig. 3-3.

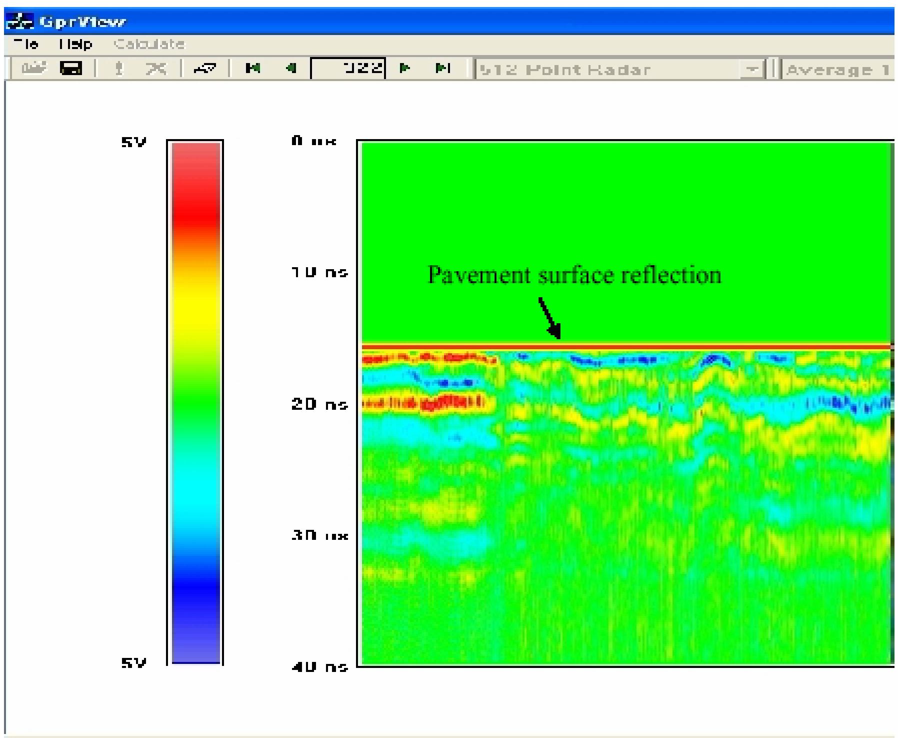

Fig. 3-3 The measured color map of Fig. 3-1 after signal processing

Compare Fig. 3-3 with Fig. 3-1. It can be seen that the interfaces of subsurface layers clearly emerge after removing the direct wave and the background noises like the vehicle reflections. By integrating the software based on the above procedures into the GPR system, an applicable air launching pulse GPR is developed.

CHAPTER 4 FIELD TESTS

In order to evaluate the properties of the developed air-coupled GPR system, a series of lab and field tests were conducted. The lab tests procedures and results are very close to that reported in the Technique Report-1 [1]. They will not be repeated in this report. The following sections will only provide some new results measured on TTI Annex, FM 2818, and Texas Avenue in College Station.

4.1 Field Tests on TTI Annex

The first field test for air-coupled GPR was carried out over the TTI Annex. The pavement is over 2000 feet long with the distance marks on side. The measurement started from the mark “0” and ended at mark “1810”; totally 1810 feet long pavement was measured. The result measured by the air-coupled GPR is given in Fig. 4-1. The software for data storing has been modified to use the data format compatible with TxDOT software. Fig. 4-1 shows the measured GPR color map in a similar style of TxDOT GPR. This result is the same as the one measured by the ground coupling GPR in [1]. From Fig. 4-1 the first asphalt layer and the second base layer are clearly seen.

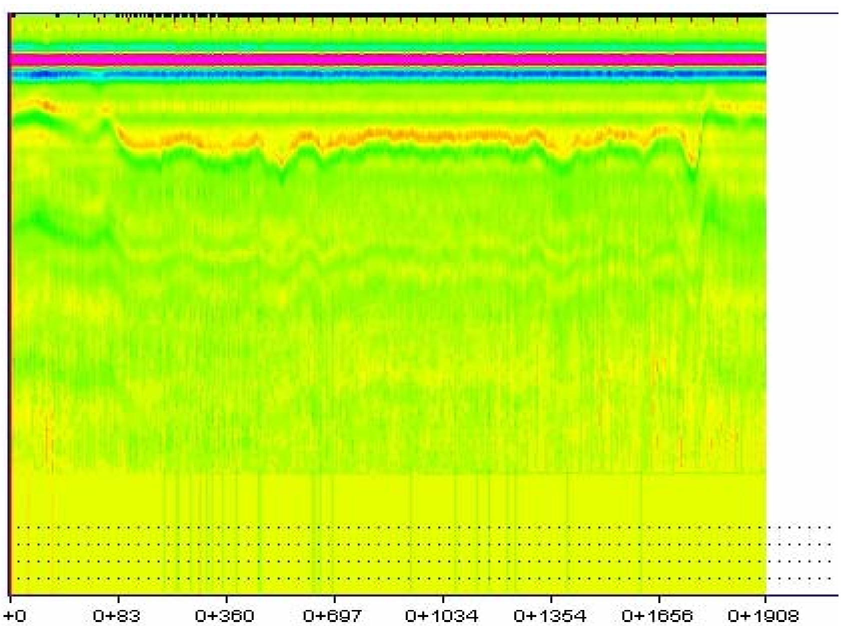

Fig. 4-1 Measured color map at TTI Annex by Air-coupled GPR

4.2 Field Tests on FM 2818 and Texas Avenue

In additional to the TTI Annex tests, more tests were also conducted on FM 2818 and Texas Avenue in College Station. Fig. 4-2 is the result measured on FM 2818 at SH60. Fig. 4-3 shows the result measured on Texas Avenue between FM 2818 and Bush Drive. The Annex data have been proven very close to that measured by TxDOT radar. In both Fig. 4-2 and Fig. 4-3, the first asphalt layer and base layers can be easily identified.

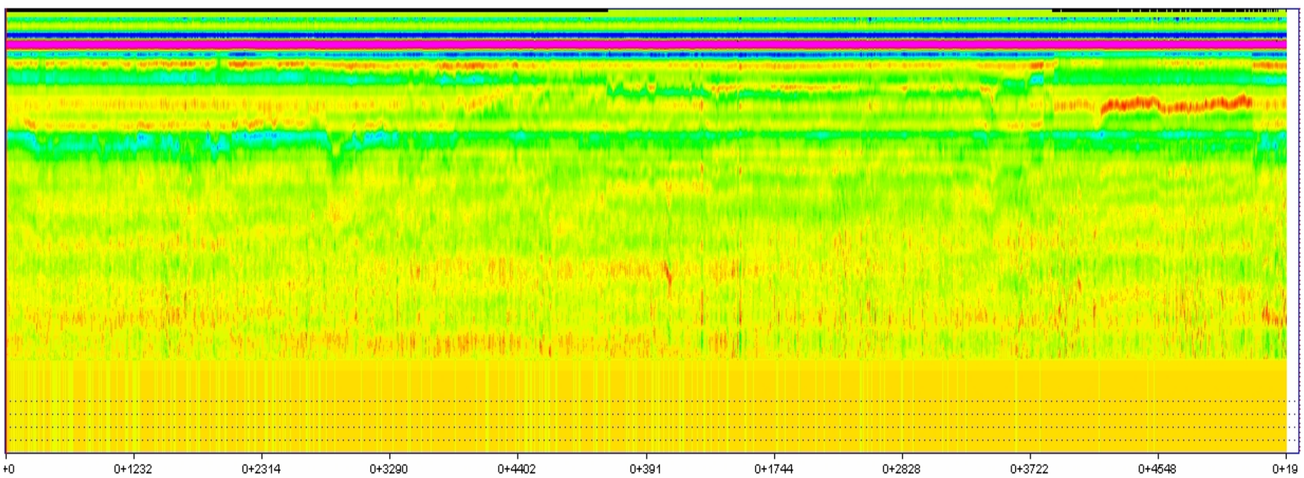

Fig. 4-2 FM 2818_SB_2mile_centered at 60

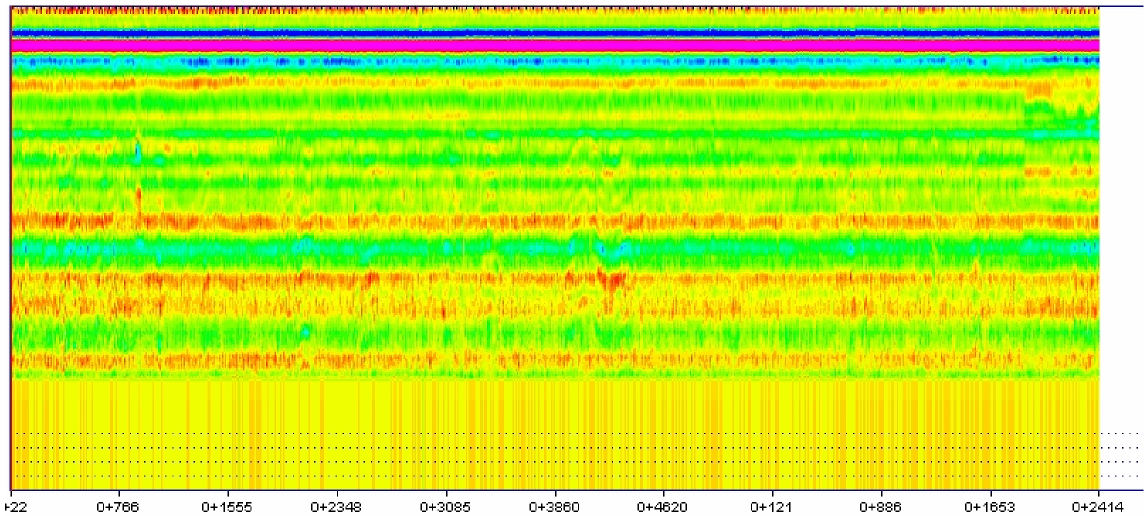

Fig. 4-3 Measured results on Texas Ave between FM2818 and Bush Dr in College Station

With the new air-coupled GPR system, all the above measurements were made in real time. No post processing was conducted.

CHAPTER 5: CONCLUSIONS AND RECOMMENDATIONS

5.1 CONCLUSIONS

A new air-coupled pulse GPR system has been successfully developed. This system is vehicle-mounted and can perform real time measurements at highway speed. It can also cooperate with vehicle DMI device to get position of each measurement. The GPR data format is compatible with TxDOT software, which benefits the information sharing and the implementation of this FCC compliant GPR system.

Lab and filed tests have been conducted on TTI Annex, FM2818, Texas Avenue, and in College Station. The measured results agree very well with the real cases.

5.2 RECOMMENDATIONS

The developed GPR system is able to collect pavement layer information accurately and in real time. The system is completely ready for implementation.

REFERENCES

[1] Liu, Richard, Li, J. and et al, "Project 04820 Technique Report – 1", TxDOT, 2006.

[2] Liu, Richard., Li, J., Gan, X., Xing, H. and Chen, X. "New Model for Estimating the Thickness and Permittivity of Subsurface Layers from GPR Data," *IEE Proc. – Radar, Sonar and Navigation*, Vol. 149, No. 6, pp315-319, December 2002.

[3] Rudolf P. Hecken, "A Near-Optimum Matching Section Without Discontinuities," IEEE Transaction on Microwave Theory and Techniques, Vol. MTT-20, No. 11, November 1972.

[4] D. A. Kolokotronis, Y. Huang and J. T. Bang, "Design of TEM Horn Antennas for Impulse Radar," 1999 High Frequency Postgraduate Student Colloquium *17* September *1999*, University *of* Leeds.

[1] A. Loulizi, *Development of Ground Penetrating Radar Signal Modeling and Implementation For Transportation Infrastructure Assessment*, Virginia Polytechnic Institute and State University, Feb 2001.

[2] S. Lahour, *Development of Data Analysis Algorithms for Interpretation of Ground Penetrating Radar Data*, Virginia Polytechnic Institute and State University, Oct 2003.

[3] A. P. Annan, *GPR Principles Procedures & Applications*, Sensors & Software Inc., Canada, 2003.

[4] http://fate.clu-in.org/gpr_main.asp

[5] http://www.lpi.usra.edu/meetings/lpsc2004/pdf/1563.pdf